AIAA-98-2507

EXPERIMENTAL STUDY OF THE MIXING OF REACTIVE GASES AT THEIR INTERFACE BEHIND A SHOCK WAVE

M. Valentino[*], *C. W. Kauffman*[†], *M. Sichel*[‡]
Department of Aerospace Engineering
The University of Michigan
Ann Arbor, MI 48109

ABSTRACT

An ongoing set of experiments is described. In these experiments the interaction of a strong plane shock wave with non-uniform gaseous mixtures are investigated. Specifically, the non-uniform mixtures examined have consisted of spherical bubbles of pure hydrogen or hydrogen-oxygen mixtures surrounded by an oxygen atmosphere. Shocks in the range of Mach 1.6 to 3.5 have been sent through the test section to interact with the non-uniform mixture. The interaction events where recorded with high speed shadowgraphs and pressure trace recordings. Rayleigh-Taylor instabilities and baroclinic torque cause the initially spherical regions to deform after passage of the shock. No chemical reaction has been observed after passage of the shock for the case of a pure hydrogen sphere immersed in an oxygen atmosphere. However, reactions have been observed for premixed hydrogen-oxygen spheres behind shocks as low as Mach 2.8. These repeatable shock-mixture interactions will aid the study of the initiation and propagation of detonation waves and provide a useful set of test data for computational fluid dynamics codes involving reactive flows.

INTRODUCTION

The interactions of shock waves with fluid non-uniformities have long been studied. Typically these studies have looked at the interface of two fluids of different densities. Such interactions are a classic example of the Rayleigh-Taylor instability caused by an acceleration field imposed on an interface of different density fluids. When the acceleration field is created by the passage of a shock wave the instability is known as a Richtmyer-Meshkov instability. Markstein [1] was the first to identify this instability experimentally. In those experiments, a shock wave interacted with a flame front causing a spike of unburned gas to penetrate into the burned gas. Richtmyer [2] provided the first analytical development showing the growth of perturbations on the interface increase linearly due to an impulsively applied acceleration. Meshkov [3] provided the first systematic experimental work to verify the linear growth rate. Brouillette & Sturtevant [4] extended this work in a series of experiments examining thick interfaces.

In all of these investigations the initial perturbations were smooth and slowly varying such that they could be represented by a sine curve. The growth rate relation for the amplitude η of the interface follows [4]

$$\frac{d\eta(t)}{dt} = \eta_0 A k \Delta U \qquad (1)$$

Where η_0 is the initial amplitude of the perturbation, A is the Atwood number, $k=2\pi/\lambda$ where λ is the wavelength of the sine perturbation, and ΔU is the change in interface velocity due to the shock. This relation holds as long as $\eta(t)<<\lambda$.

In addition to studying the shock-induced instabilities at the interface of different density media, one can also examine the shock reflection and refraction at the interface. Abd-el-Fattah, Henderson, & Lozzi [5] and Catherasoo & Sturtevant [6] conducted investigations of shocks interacting with planar interfaces. Haas & Sturtevant [7] extended this work by looking at shock interactions with cylindrical and spherical interfaces. Their experimental images clearly show the initial

[*] Graduate Research Assistant, Member AIAA

[†] Professor, Member AIAA

[‡] Professor, Member AIAA

deformations of the test volumes due to Rayleigh-Taylor instabilities and also show how vortical structures appear as time progresses.

One of the first analytical treatments describing the deformation process leading to vortex rings was done by Rudinger & Somers [8]. He broke the process into two stages. In the first stage the bubble is impulsively accelerated by the shock with little deformation. The second stage consisted of the vortex formation, which he modeled as a vortex formed by an impulsively moved disk. In addition to the analytical treatment in Ref. [8], there are experimental images of a flame bubble in the beginning stages of forming into a vortex ring. Interestingly, these images were attributed to unpublished work of Markstein.

The vorticity generation in these bubbles due to a shock passage can easily be explained by examining the vorticity equation

$$\rho \frac{D}{Dt}\left(\frac{\vec{\omega}}{\rho}\right) = (\vec{\omega}\cdot\nabla)\vec{u} + \frac{1}{\rho^2}(\nabla\rho\times\nabla p) \qquad (2)$$

The second term on the right shows that vorticity, $\vec{\omega}$, will be generated whenever the density and pressure gradients are not aligned. This term is known as the baroclinic torque.

The case of a shock passing over a cylindrical volume of less dense gas surrounded by a heavier gas is depicted in figure 1a. As the shock proceeds across the test volume vorticity is deposited along the interface of the two gases. The maximum vorticity is generated when the density and pressure gradients are at ninety degrees corresponding to the top and bottom of the cylinder represented in figure 1b. The result is that the vorticity tends to deform the cylinder into a kidney shape shown in figure 1c and eventually into a pair of vortex lines.

By extension it is easily seen that a spherical bubble would tend to form into a vortex ring. As time progresses even further, the original vortex ring induces the formation of a second vortex ring. As shown schematically in figure 2, the first vortex ring creates a re-entrant jet at the centerline of the bubble. As the jet pierces the upstream edge of the sphere it will spread out laterally and form into a second vortex ring ahead of the original. The first experimental evidence of the second ring and description of the formation process was provided by Haas & Sturtevant [7].

For the most part the research cited above have looked at the interaction of relatively weak shock waves and inert gases. The thrust of the present work is to make the extension to stronger shock waves and to consider the interaction of the shocks with chemically reactive gases.

Consider spherical bubbles of pure hydrogen immersed in an oxygen atmosphere. As a shock passes over the hydrogen bubble the baroclinic torque mechanism will create a pair of vortex rings and lead to a mixing of the hydrogen and oxygen. The mixing coupled with the increased pressure and temperature behind the shock wave can lead to conditions were chemical reaction might take place. The goal of this work is to determine the conditions under which an un-premixed hydrogen-oxygen system will lead to chemical reaction.

EXPERIMENTS

These experiments are being conducted in the shocktube shown schematically in figure 3. The shock tube has a rectangular cross section with internal dimensions of 64 x 38mm and is approximately 8m long. Mylar diaphragms are used to separate high-pressure helium in the driver section from the remainder of the tube. The diaphragms have a thickness of 0.2mm and are stacked together in various numbers depending on the desired shock strength. The test-section, located approximately 4.5m downstream of the diaphragms, has removable glass windows that allow a 200 x 50mm field of view.

Pulsed laser shadowgraphs are used to capture the shock interactions with the test gas spheres through the glass windows located in the test section. The pulsed laser system, shown in figure 4, consists of a Spectra Physics argon-ion laser model 2020 coupled with a cavity-dumper model 334. A gated pulse frequency signal is sent to the cavity-dumper to control the number and frequency of images taken during a run. Typically the laser is set to pulse for 400μs with a pulse width of 9ns and a pulse separation of 2 to 20μs providing up to 35 frames of the interaction process per run. A Cordin streak camera is used to capture the images on a strip of 70mm x 300mm Kodak pan film 2484.

Along with the shadowgraph system a series of pressure switches are located upstream of the test

section. These are used to give shock velocity measurements and initiate the laser pulse system. In addition to the pressure switches, two pressure transducers located inside the test section are used to provide pressure traces during the interaction process. Finally, a fast response photo detector was aimed through the test section windows at the test gas spheres. The diode used can resolve individual light flashes on the order of 1 microsecond. The detector was to record any light emissions that would indicate a chemical reaction taking place.

To prepare for an experimental run the entire shock tube is first evacuated and then filled with oxygen at one atmosphere. The test gas spheres are constrained within a soap bubble that is supported on its bottom by a post located in the middle of the test section. The cylindrical post is stainless steel tubing with a 3.2mm outer diameter and a 0.7mm inner diameter. A small piece of paper with a pinprick in the center is placed on top of the post to keep the soap drop from running down the interior before the gas sphere is made. The spheres are then made using a gas tight syringe to inject the test gas from the bottom of the post. The test section was designed with small ports directly above and below the post to allow the depositing of the soap drop and injection of the test gas after the shock tube has been filled with oxygen. All test gas spheres created were on the order of 6cc in volume and 19mm in diameter. The diaphragms are ruptured as quickly as possible after the bubble is created to minimize the diffusion of hydrogen into oxygen at the soap bubble interface. The typical time from when the bubble is created until the shock interaction is less than one minute.

DISCUSSION

Pure Hydrogen Bubbles

The first series of tests looked at bubbles of pure hydrogen immersed in an oxygen atmosphere. The range of Mach numbers investigated ran from 1.6 to 3.51. A test matrix of the experimental conditions run to date are shown in table 1.

Table 1. Shock Tube Test Matrix, Pure Hydrogen Bubbles

Shock Wave Mach Number	Test Volume Gas	Indication of Chemical Reaction
1.60	H_2	No
2.70	H_2	No
2.78	H_2	No
2.96	H_2	No
3.41	H_2	No
3.51	H_2	No

Figure 5 shows the series of shadowgraph images taken of the Mach 1.6 shock interacting with the pure hydrogen bubble. The images are taken 6μs apart for a total elapsed time of 192μs. These images clearly show how the bubble transformed into a pair of vortex rings. The camera's external shutter not being fully open caused the dark area on the left-hand side of the images up through 72μs. The four dark vertical lines at the left hand of the images are due to a series of grooves on the test section's glass windows. These were ground into the glass for a future set of experiments, but are useful in these tests as reference marks. 25.4mm separate all four from each other.

Selected frames from figure 5 are enlarged and repeated in figure 6 for clarity. At time zero the incident shock wave moving from the left has just reached the hydrogen bubble. Two transverse waves can be seen following the incident shock. These waves are probably caused by slight misalignments of a joint between the test section and the main shock tube.

By 18μs the incident shock has reached the middle of the original bubble. The left-hand side of the bubble has been deformed due to the incident shock and a reflected wave can be seen emanating from that side. The refracted wave can be seen running ahead of the incident shock inside the bubble. This occurs because the speed of sound of hydrogen is higher than that of the surrounding oxygen.

As the refracted wave encounters the right hemispherical interface it creates both a transmitted wave that now moves into the oxygen and an internally reflected wave. The internally reflected wave will eventually create a secondary transmitted wave that exits from all sides of the bubble. At 36μs the transmitted wave has emerged entirely from the

upstream edge of the bubble. The secondary transmitted wave can be seen emerging at the top of the bubble behind the diffracted leg of the incident shock. A bow shock has also formed in front of the bubble support post.

The apparent thickening of the transmitted shock directly ahead of the bubble in the images from 36 to 72μs is an optical illusion due to two factors. The first is that the shadowgraphs are a 2-dimensional projection of a 3-dimensional volume. The second is due to the fact that the "wave" in this area is actually comprised of three waves in close proximity. The first wave is the transmitted wave, which is closely followed by the secondary transmitted wave. Both of these waves are trailed by the incident shock as it diffracts around the upstream interface of the bubble. Because of the 3-D effects and the image size the three waves can not be resolved separately in these shadowgraphs.

At 90μs the re-entrant jet has just pierced the leading edge of the bubble and has begun to spread laterally. The bubble's shape is now close to that depicted in figure 2a. By 192μs the second vortex ring is well defined and has actually become larger than the initial ring.

These results are qualitatively very similar to the Mach 1.25 shock interacting with a helium sphere presented by Haas & Sturtevant [7]. One interesting difference is that the Mach 1.6 case presented here develops into the dual vortex rings on the order of 3 to 4 times faster. Also, in Haas & Sturevant's case the second vortex ring never grows larger than the first and tends to separate or move ahead of the first vortex by quite a distance. The most likely explanation of the differences is the flow behind the Mach 1.25 shock is low subsonic while that behind the Mach 1.6 case at hand is supersonic. Also to be considered is that the bubbles of Haas & Sturtevant were twice the size as the present work and consisted of helium in air as opposed to hydrogen in oxygen. Further analysis needs to be completed in this area.

Figure 7 shows the series of shadowgraph images taken of the Mach 2.96 shock interacting with a pure hydrogen bubble. These images are taken every 12μs apart for a total time of 192μs. It is evident that for this case the hydrogen bubble is convected downstream roughly twice as fast as the Mach 1.6 case. There is also no clear indication of the formation of a second vortex ring. However, the bubble does seem to broaden slightly beginning at 132μs. This may be due to a re-entrant jet spreading laterally at the downstream edge of the bubble. Unfortunately, the bubble is convected out of the field of view too quickly to see if a second vortex ring does develop.

In addition to seeing no second vortex ring, there is no evidence of any chemical reaction of the hydrogen and oxygen. The pressure and temperature behind a Mach 2.96 shock should be close to that needed for the auto-ignition of a premixed H_2/O_2 system. In order to see a chemical reaction for the un-premixed case at hand, the pressure and temperature must remain at an elevated level long enough for sufficient mixing to take place along with the required induction time of the H_2/O_2 reaction. Because the bubble does seem to remain closely coupled to the incident shock, there most likely has not been sufficient mixing for a chemical reaction to occur. It is possible that the correct conditions occur after the bubble has passed out of the field of view.

Shocks of Mach 3.41 and 3.51 interacting with pure hydrogen bubbles were also investigated. The results were similar to those of the Mach 2.96 case with no chemical reactions observed.

Premixed Bubbles of H_2/O_2

Although no chemical reactions were seen for any "clean" runs of the pure hydrogen bubbles, on several "bad" runs a reaction was observed. The indicators of a chemical reaction were a flash of light detected by the photometer and strong pressure waves seen emanating from the bubble on the shadowgraph images. The "bad" runs happened when it took an excessive amount of time between the creation of the test gas bubble and the shock or when many small bubbles of the hydrogen gas would form around the bottom of the main bubble. Both of these cases represent some degree of premixing of the hydrogen and oxygen before the shock arrives. For the long time delays, on the order of eight to ten minutes, a hydrogen bubble originally 19mm in diameter will shrink to a diameter of 16mm and will therefore have a region of premixed gas surrounding the now smaller bubble. For the cases of small bubbles forming under the main bubble it is likely the small bubbles rupture and mix quickly after the shock passes allowing ignition to occur.

Encouraged by the results of these "bad" runs, it was decided to make some controlled runs of premixed hydrogen-oxygen bubbles. To date several runs of both stoichiometric mixtures and mixtures with an equivalence ratio of 0.7 have been investigated. A test matrix of experimental conditions run to date along with an indication of chemical reaction observed are shown in table 2. Reactions have been observed for shock Mach numbers as low as 2.92 for stoichiometic mixtures and 2.84 for mixtures at an equivalence ratio of 0.7.

Table 2. Shock Tube Test Matrix, Premixed Hydrogen-Oxygen Bubbles

Shock Wave Mach Number	Test Volume Gas	Indication of Chemical Reaction
2.82	Stoichiometric H_2/O_2	No
2.92	Stoichiometric H_2/O_2	Yes
3.33	Stoichiometric H_2/O_2	Yes
2.53	H_2/O_2 , $\phi = 0.7$	No
2.84	H_2/O_2 , $\phi = 0.7$	Yes
3.08	H_2/O_2 , $\phi = 0.7$	Yes

Figure 8 shows the series of shadowgraph images taken of the Mach 3.08 shock interacting with a premixed bubble of H_2/O_2 at an equivalence ratio of 0.7. An oxygen atmosphere surrounds the premixed bubble. The interaction process appears the same as non-reacting runs up through 36μs. Somewhere between 36 and 48μs chemical reaction has begun. A strong blast wave is clearly seen at 48μs. This wave appears to support the incident shock which shows signs of curvature. The curvature of the incident shock is more clearly seen at 60 and 72μs as the blast wave has grown to fill the test section from top to bottom. At 72μs a reflected wave can be seen under the bubble from the blast wave encountering the bottom of the test section.

SUMMARY & RECOMMENDATIONS

The interaction of strong shock waves with isolated regions of hydrogen and hydrogen/oxygen mixtures are being investigated in an ongoing series of experiments. The wave pattern results for a spherical bubble of pure hydrogen behind a shock of Mach 1.6 are qualitatively similar to the results of Haas & Sturtevant [7] for a helium bubble behind a shock of Mach 1.25. However at Mach 1.6, the dual vortex ring system develops 3 to 4 times as fast and the second ring grows larger than the first.

No chemical reactions have been observed in the interactions of shocks with strengths up to Mach 3.51 with pure hydrogen spheres. The lack of chemical reactions is due to inadequate mixing of the hydrogen and oxygen in the time periods investigated. When bubbles of premixed hydrogen and oxygen are subjected to the same strength shocks chemical reaction has been observed.

The chemical reactions behind the premixed bubbles are identified by the presence of strong blast waves appearing the shadowgraph images. Further analysis is required to determine the strength of the blast waves and the extent to which they support the incident shock wave.

ACKNOWLEDGMENTS

This work was supported by the Wright Laboratory Armament Directorate and the PALACE KNIGHT program of the United States Air Force.

REFERENCES

1. Markstein, G. H. 1957 A shock tube study of flame front-pressure wave interaction. *Sixth Symp. (Intl) on Combustion*, pp 387-390. Reinhold

2. Richtmyer, R.D. 1960 Taylor instability in shock acceleration of compressible fluids. *Commun. Pure Appl. Maths* **23**, 297-319

3. Meshkov, E.E. 1969 Instablility of the interface of two gases accelerated by a shock wave. *Izv. AN SSSR. Mekhanika Zhidkosti i Gaza*, Vol. 4, No. 5, 151-157

4. Brouillette, M. & Sturtevant, B. 1994 Experiments on the Richtmyer-Meshkov instability: single perturbations on a continuous interface. *J. Fluid Mech.* **262**, 271-291

5. Abd-El-Fattah, A.M., Henderson, L.F. & Lozzi, A. 1976 Precursor shock waves at a slow-fast gas interface. *J. Fluid Mech.* **76**, 157-176

6. Catherasoo, C.J. & Sturtevant, B. 1983 Shock dynamics in non-uniform media. *J. Fluid Mech.* **127**, 539-561

7. Hass, J.F. & Sturtevant, B. 1987 Interaction of weak shock waves with cylindrical and spherical gas inhomogeneities. *J. Fluid Mech.* **181**, 41-76

8. Rudinger, G. & Somers, L.M. 1960 Behavior of small regions of different gases carried in accelerated gas flows. *J. Fluid Mech.* **7**, 161-176

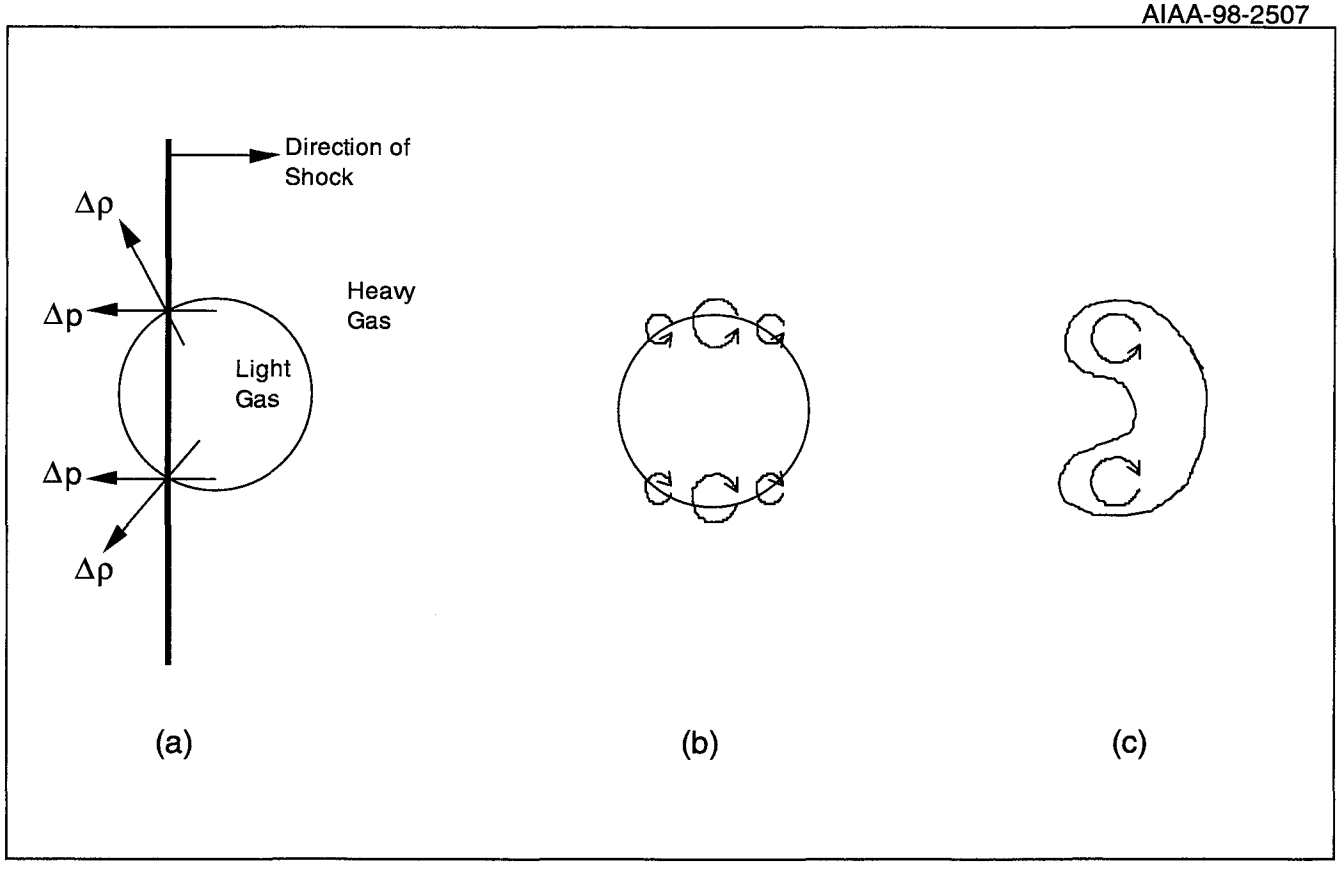

Figure 1: Shock interacting with a region of light gas: (a) Schematic of the baroclinic torque mechanism. (b) Vorticity deposited along the interface. (c) Deformation of the light gas region.

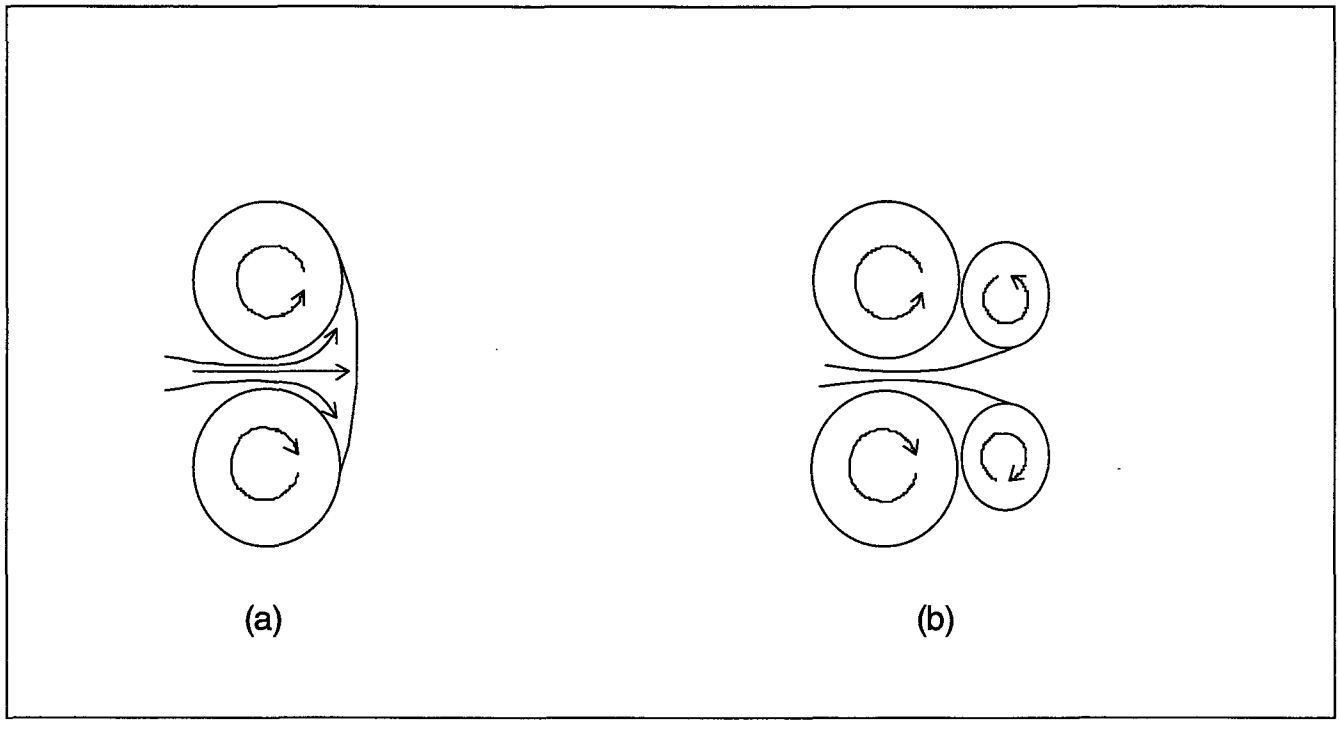

Figure 2. Schematic of development of a second vortex ring: (a) Re-entrant jet piercing upstream edge and spreading laterally. (b) Dual vortex ring formation

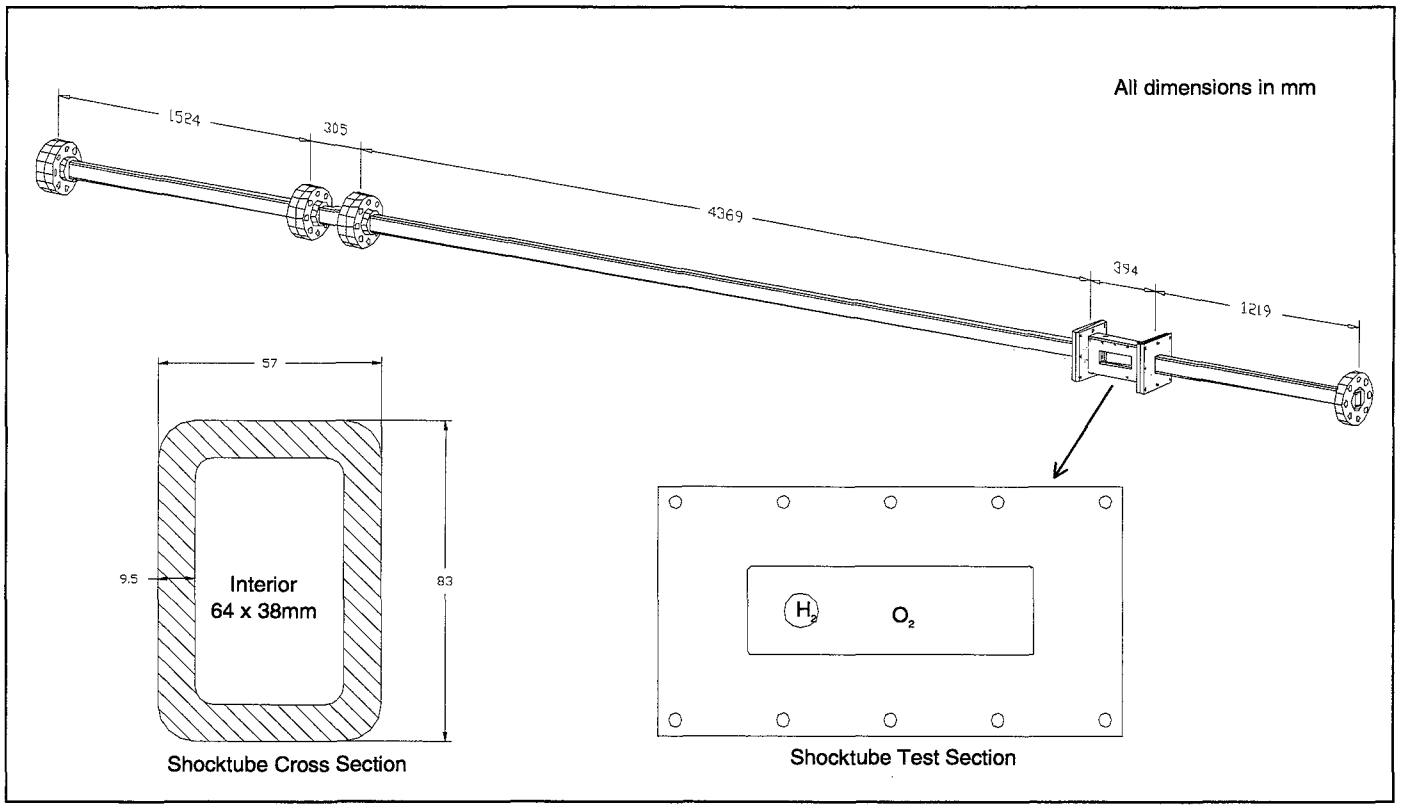

Figure 3. Shock tube schematic

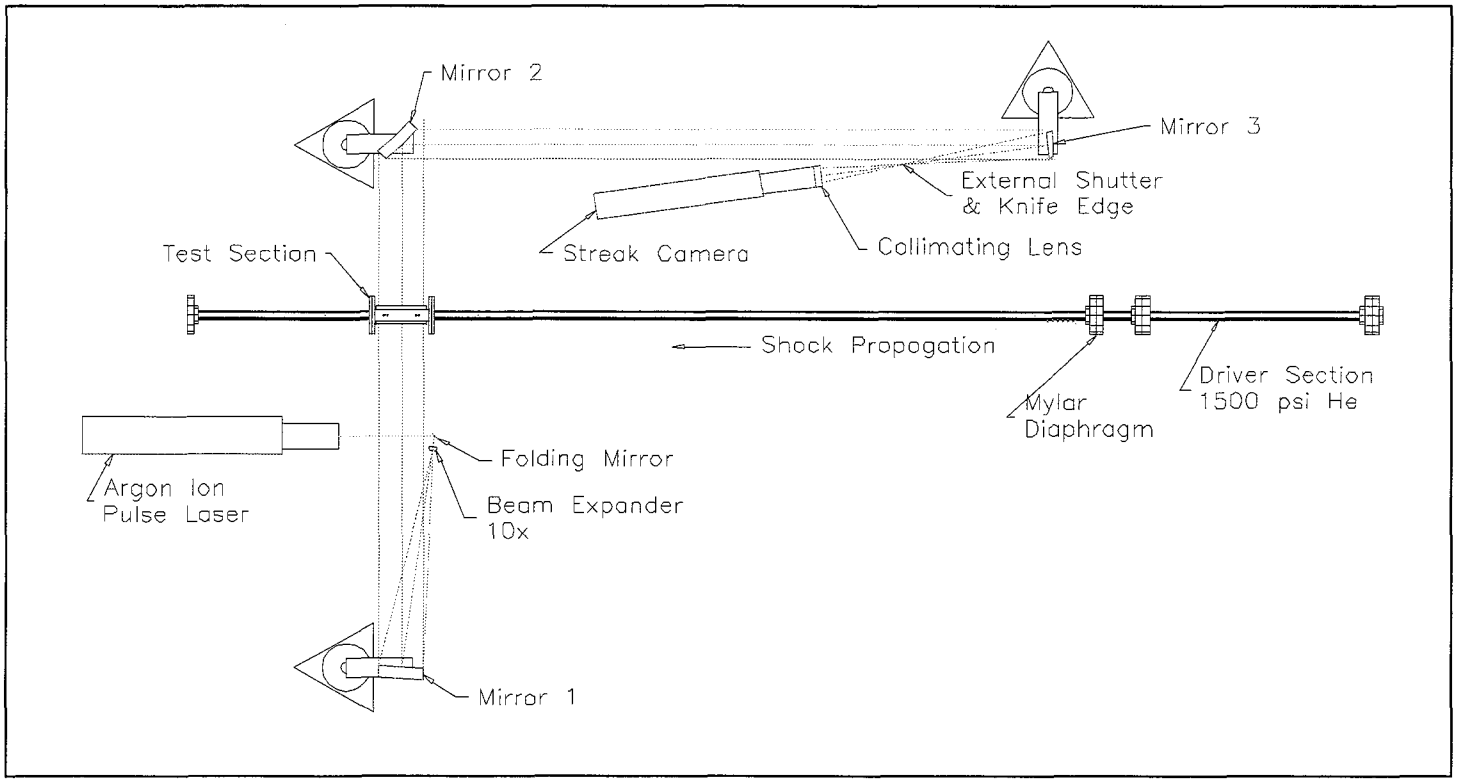

Figure 4. Pulsed laser shadowgraph system.

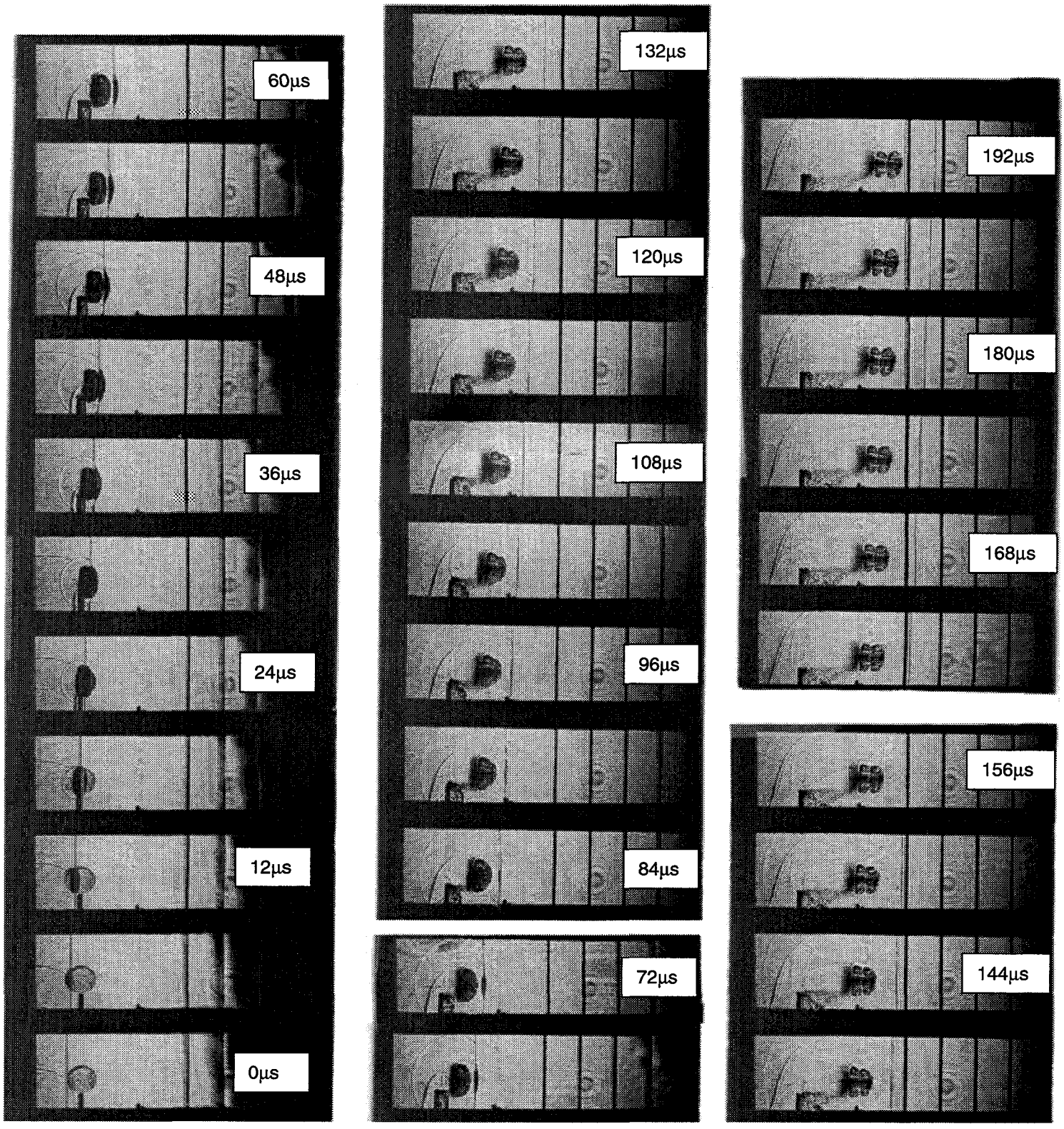

Figure 5: Shadowgraphs of a Mach 1.6 shock interacting with a spherical hydrogen bubble in an oxygen atmosphere. 6μs between frames (note: image at 78μs is not shown).

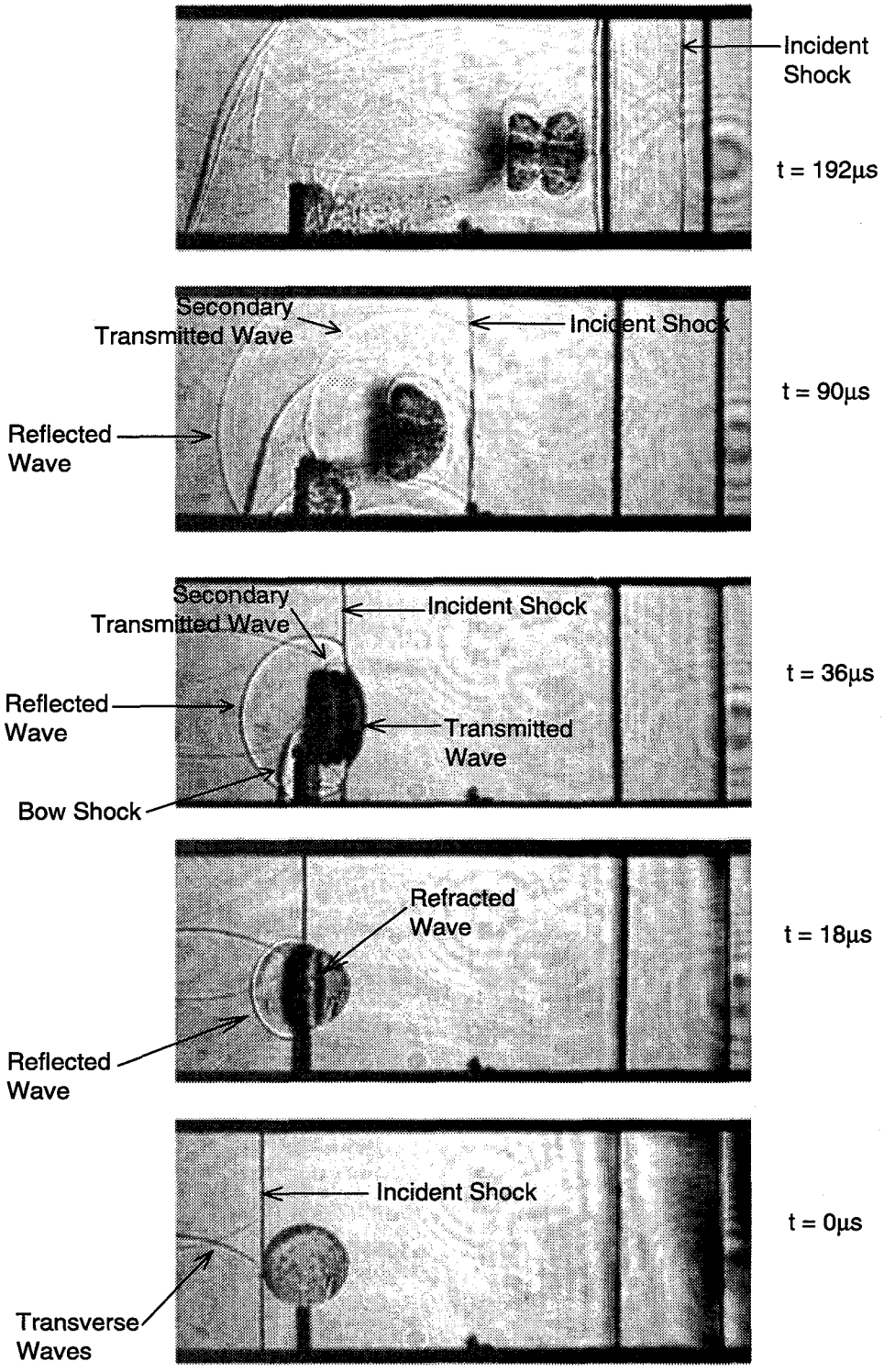

Figure 6: Selected shadowgraphs of a Mach 1.6 shock interacting with a spherical hydrogen bubble in an oxygen atmosphere.

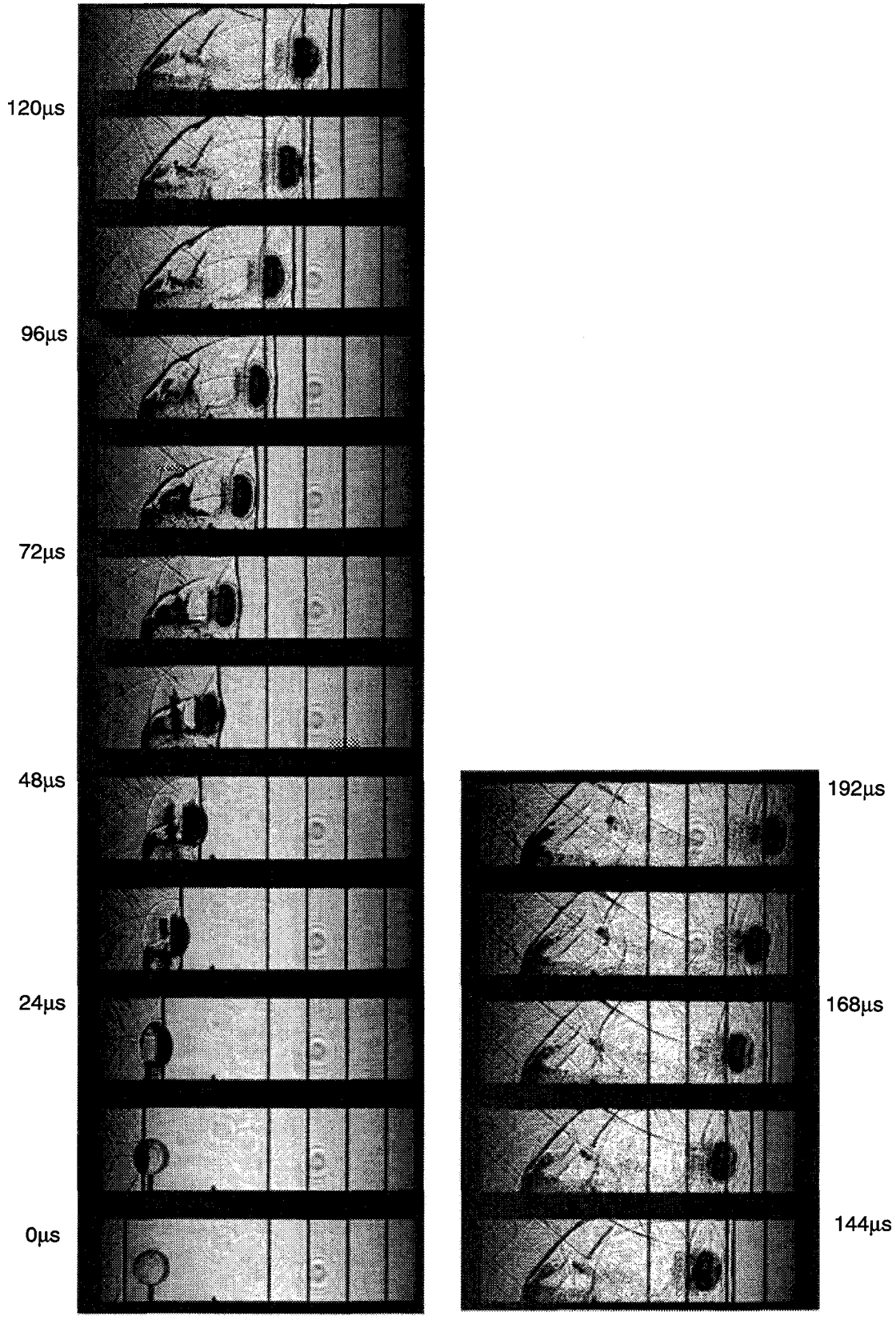

Figure 7: Shadowgraphs of a Mach 2.96 shock interacting with a spherical hydrogen bubble in an oxygen atmosphere. 12μs between frames.

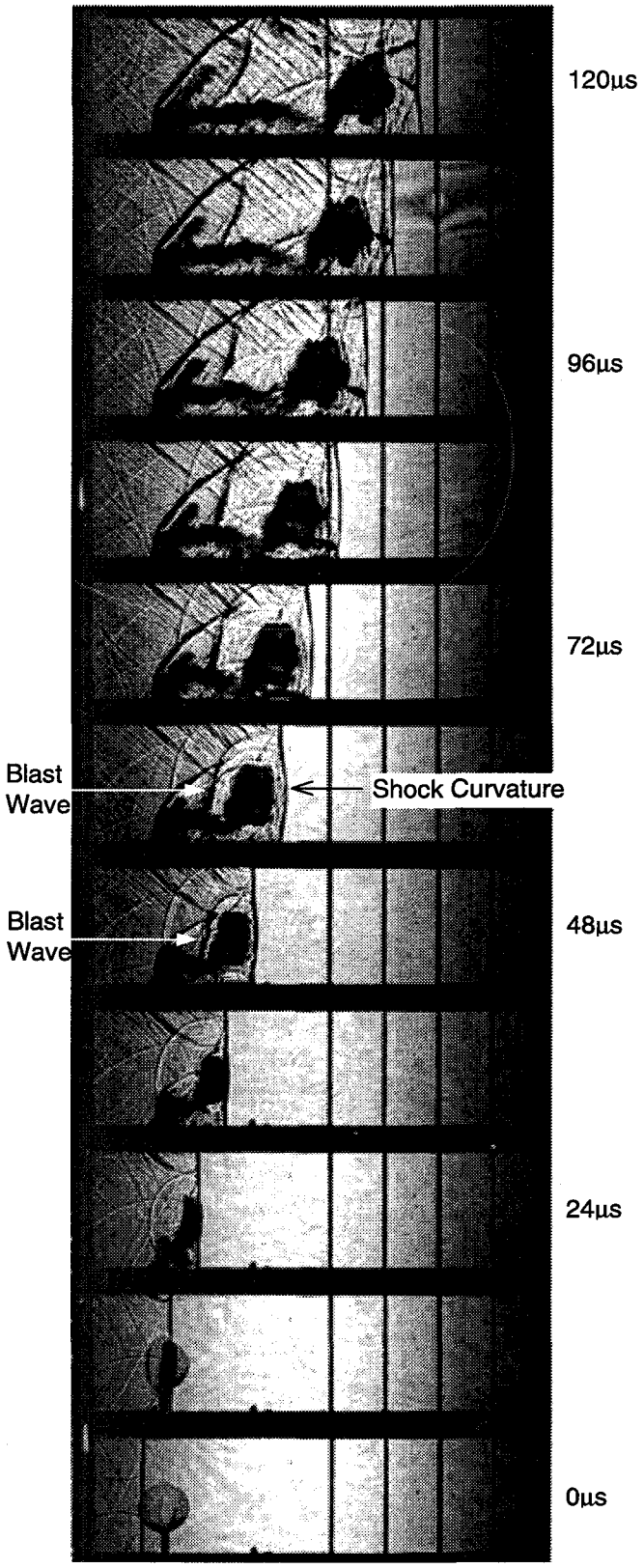

Figure 8: Shadowgraphs of a Mach 3.08 shock interacting with a spherical hydrogen/oxygen with an equivalence ratio of 0.7 surrounded by an oxygen atmosphere. 12μs between frames.